Theoretical Notes
Note 242

UNCLASSIFIED
SECURITY CLASSIFICATION OF THIS PAGE (When Data Entered)

REPORT DOCUMENTATION PAGE

READ INSTRUCTIONS BEFORE COMPLETING FORM

1. REPORT NUMBER: HDL-TR-1735	2. GOVT ACCESSION NO. / 3. RECIPIENT'S CATALOG NUMBER
4. TITLE (and Subtitle): Formation of a Nonuniform Conducting Region near an Air-Solid Boundary during Irradiation by a Pulse of High Energy Electrons	5. TYPE OF REPORT & PERIOD COVERED: Technical Report
	6. PERFORMING ORG. REPORT NUMBER
7. AUTHOR(s): Herschel Weil (William T. Wyatt, Jr., HDL contact)	8. CONTRACT OR GRANT NUMBER(s): DRCMS: 612118.11.H7500, DRCMS: 697000.22.11467
9. PERFORMING ORGANIZATION NAME AND ADDRESS: Harry Diamond Laboratories, 2800 Powder Mill Road, Adelphi, MD 20783	10. PROGRAM ELEMENT, PROJECT, TASK AREA & WORK UNIT NUMBERS: Program: 6.27.04, Task: B088, Work Unit: 61
11. CONTROLLING OFFICE NAME AND ADDRESS: Director, Defense Nuclear Agency, Washington, DC 20305; Commander, US Army Materiel Development & Readiness Command, Alexandria, VA 22333	12. REPORT DATE: January 1976
	13. NUMBER OF PAGES
	15. SECURITY CLASS. (of this report): UNCLASSIFIED
	15a. DECLASSIFICATION/DOWNGRADING SCHEDULE

16. DISTRIBUTION STATEMENT (of this Report)

Approved for public release; distribution unlimited.

17. DISTRIBUTION STATEMENT (of the abstract entered in Block 20, if different from Report)

18. SUPPLEMENTARY NOTES

HDL Project: X755E3, E055E3
This work was partially funded under AMC NWER/T and by the Defense Nuclear Agency under its Subtask R99QAXEB088, "EMP Interaction and Coupling," Work Unit 51, "Source-Region Coupling."

19. KEY WORDS (Continue on reverse side if necessary and identify by block number)

Plasma
Plasma sheath
Method of characteristics

20. ABSTRACT (Continue on reverse side if necessary and identify by block number)

Equations are presented to describe the formation of the nonuniform plasma that will be generated on the air side of an air-solid interface by secondary electrons, due to a time-varying flux of Compton electrons. For tractability of the equations, a one-dimensional geometry is used. The equations are then a set of coupled nonlinear hyperbolic

DD FORM 1 JAN 73 1473 EDITION OF 1 NOV 65 IS OBSOLETE

UNCLASSIFIED
SECURITY CLASSIFICATION OF THIS PAGE (When Data Entered)

partial differential equations for the densities and velocities of the secondary electrons and ions and the electric field, in terms of two independent variables: time and perpendicular distance from the interface. An interactive numerical procedure is outlined for stepwise simultaneous determination of both the characteristics (which depend on the solutions because of the nonlinearity) and the solutions to the equations.

CONTENTS

FIGURES

1. INTRODUCTION

1.1 The General Problem

When a stream of high-energy electrons, such as the Compton recoil electrons generated by a gamma-ray flux, penetrates nonionized air of approximately sea-level density, the air is ionized by emission of secondary electrons; it becomes a partly ionized plasma. Two currents maintain an electromagnetic field in the medium: the incident current plus a current due to motion of the secondary electrons and their associated positive ions plus negative ions caused by attachment of electrons to O_2. The electric field may be thought of as related to the secondary currents by a conductivity, σ, which then characterizes the macroscopic electrical properties of the plasma.

Near any solid boundary, a boundary layer or sheath of nonuniform σ exists. One can draw an analogy to the nonuniform electron-deficient sheath that forms around any object (e.g., an antenna or a dc probe) inserted into an already existing plasma. The currents, which such probes draw from the plasma as a function of dc bias relative to the distant plasma, and their effective ac input impedances are sensitive functions of the sheath structure.[1] Hence, to determine how effectively an object immersed in a plasma couples to incident radiation (therefore, how much power gets into interior circuitry), it is necessary to know the sheath structure. This is the motivation behind the present analysis: we formulate a system of equations governing the plasma formation near a wall due to an incident pulse of high-energy electrons and then develop a scheme for its numerical solution.

1.2 A Model Problem for Analysis

The most general sheath problems that have been attacked in the literature deal with determining the steady-state or quasi-static sheath structure and single-frequency, small, ac perturbations of this structure.[2] Transient analyses involving formation of the ambient plasma very near a boundary have not been carried out. To analyze these steady-state problems, it has been necessary to deal with very simple geometries. Hence, for the present more complex problem, consider the simplest possible geometry: an infinite plane boundary separating two half spaces, one of air and one of a material medium that is specified

---

[1] *J. Tarstrup and W. D. Heikkila, The Impedance Characteristic of a Spherical Probe in an Isotropic Plasma, Radio Science, 7 (April 1972), 493-502.*

[2] *J. D. Swift and M. J. R. Schwar, Electrical Probes for Plasma Diagnostics, American Elsevier, New York (1972).*

simply by fixed values of conductivity σ, permittivity ε, and permeability $\mu = \mu_o$. The time-varying incident high-energy electron flux is taken to be normal to the interface, so the entire problem is one dimensional. Two cases, (a) incidence from the air side and (b) incidence from the material side, are considered as shown in figure 1(a, b). Together they should permit one to handle the more realistic problem of a finite thickness slab as shown in case c (fig. 1(c)).

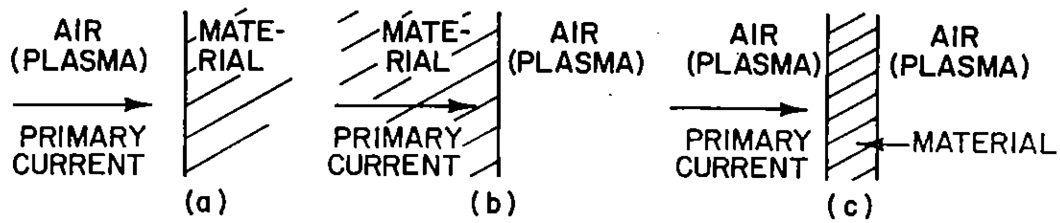

Figure 1. Different cases treated.

For the conditions to be treated here, the air is never strongly ionized, so that momentum interchange by collisions as it affects charged-particle velocities is predominantly through charged particle-neutral collisions. The mean free path for such collisions, ℓ, and the Debye length, λ_D, both measured far from the wall, are such that $\ell << \lambda_D$. Under such conditions, the steady-state analyses show that the sheath thickness extends from a few to several Debye lengths, depending on the potential of the wall relative to the potential far from the wall. Thus, the highly nonuniform region (the region of interest) on the air side in this problem is of a fairly limited thickness. Thus, it is reasonable to expect to work out solutions to this problem by numerical integrations of the differential equations.

2. THE EQUATIONS

2.1 Source Term

The source current density of high-energy electrons is taken to be $\hat{z}$ directed and of the form

$$J = J_o\left(t - \frac{z}{c}\right)\exp(-\gamma z)\hat{z} \tag{1}$$

where $J_o(t) = 0$, $t < 0$, and is continuous and has a continuous first derivative for $t > 0$. γ and c are positive constants, c being close to the velocity of light and $\gamma \sim \rho/30$,[3] where ρ is the mass density of the medium in grams per cubic centimeter. The theory does not rest on the exact choice of $J_o(t)$, but the function used will be one such as

$$J_o(t) = J_m \cdot \left(\frac{t}{\tau}\right)\exp\left(1 - \frac{t}{\tau}\right), \quad t \geq 0$$
$$= 0 \qquad\qquad\qquad , \quad t < 0 . \tag{2}$$

This function is sketched in figure 2.

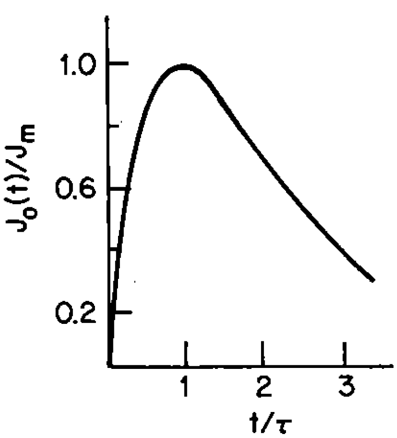

Figure 2. Model of current pulse.

2.2 Electromagnetic Fields in the Plasma

With the boundary equation and the source current both depending on z only, the electric field excited by the primary current must have the form

$$\bar{E}_p = E_p(z)\hat{z} .$$

[3]*C. L. Longmire, Direct Interaction Effects in EMP, Air Force Weapons Laboratory Interaction Notes EMP 305 IN 69, Section 5 (1974).*

The initial injection velocities of the secondary particles are mainly transverse to $\hat{z}$ with no preferred direction in the transverse plane. Since the primary current and field are z directed, the secondaries quickly pick up a z-directed drift resulting in an induced z-directed secondary current density $J_s \hat{z}$. Based on these ideas, total $\bar{E}$ due to primary and secondary currents is assumed to be $\hat{z}$ directed,

$$\bar{E} \approx E(t,z)\hat{z} \ ,$$

so that $\bar{E}$ has zero curl. Then Maxwell's equations become

$$\frac{\partial \bar{B}}{\partial t} = 0 \ , \qquad \text{curl } \bar{B} = \mu_o \left(J + J_s + \varepsilon_o \frac{\partial E}{\partial t} \right) \hat{z} \quad . \tag{3}$$

One assumes that there is no initial $\bar{B}$ field; hence, $\bar{B}$ and curl $\bar{B}$ are always zero. Then the total conduction current is equal and opposite to the vacuum displacement current and

$$E(t,Z) = - \varepsilon_o^{-1} \int_o^t \left[J(u,z) + J_s(u,z) \right] du \ . \tag{4}$$

2.3 Conservation Equations

To determine the secondary current, one must set up the equations governing the generation and motion of the secondary electrons and ions that are produced by collisions of the primary electrons with air molecules. Also, one must allow for possible subsequent attachment of secondary electrons to O_2 and for electron-ion recombination.

Define n_α and $\bar{u}_\alpha$ as the density and velocity of the αth charged particle species; α = e (electron), + (positive ion), - (negative ion). The equations for conservation of charge are

$$\text{div}\left(n_e \bar{u}_e\right) + \frac{\partial n_e}{\partial t} = S - \breve{\alpha} n_e - \breve{\varepsilon} n_+ n_e \tag{5}$$

$$\text{div}\left(n_- \bar{u}_i\right) + \frac{\partial n_-}{\partial t_+} = \breve{\alpha} n_e - \breve{\beta} n_+ n_- \tag{6}$$

$$\text{div}\left(n_+ \bar{u}_+\right) + \frac{\partial n_+}{\partial t} = - \breve{\beta} n_+ n_- - \breve{\varepsilon} n_+ n_e + S \ . \tag{7}$$

In these equations, S is the source function for secondary electrons (and is related to J below). The coefficient for electron attachment to O_2 is $\alpha(\sim 10^8\ s^{-1}$ at sea level) and the recombination coefficents

$$\breve{\varepsilon} \sim \breve{\beta} \approx 2 \times 10^{-6} cm^3/s \ .$$

If it were not for the divergence terms, these equations would express the statement that the number of positive particles equals the number of negatives. This is, in fact, not true near the boundary for a number of reasons, including that the mobilities of electrons and ions differ, the material in the wall may more efficiently neutralize incoming positive ions than electrons or negative ions, and the source term S depends on distance from the boundary for points close to the boundary.

In keeping with our earlier remarks, the ordered (average) velocity of secondaries is z directed. Use of equations (5) to (7) implies that the newly formed secondaries immediately take up the local

$$\bar{u}_\alpha = u_\alpha(t,z)\hat{z} \ .$$

Then

$$\text{div } n_\alpha \bar{u}_\alpha = \partial\left(n_\alpha u_\alpha\right)/\partial z$$

may be used in equations (5) to (7).

Finally, equations (5) to (7) imply an essentially infinite supply of neutrals, i.e., a very low percentage of ionization. Therefore, a fourth equation governing the variation in neutral density is not needed.

The three particle velocities u_α are obtained with the help of the equations of conservation of momentum,

$$\frac{\partial u_\alpha}{\partial t} + u_\alpha \frac{\partial u_\alpha}{\partial z} = \frac{q_\alpha}{m_\alpha} E - \frac{1}{n_\alpha m_\alpha} \text{grad } p_\alpha - \nu_\alpha u_\alpha \ . \qquad (8)$$

Here, ν_α is the particle-neutral collision frequency, and q_α, m_α, and p_α are charge, mass, and partial pressure of the αth species.

Equation (8) is based on several implicit assumptions. The low percentage of ionization was used to justify neglect of momentum interchange between charged particles. Also, no Lorentz force term $q_\alpha(\bar{u}_\alpha \times \bar{B})$ is included. Although there is no time-varying $\bar{B}$, there does exist the static geomagnetic field, so omitting the Lorentz force needs some justification.

In the simpler instance, where all production and loss terms are neglected and there are no transient or boundary effects, inclusion of $\bar{u}_\alpha \times \bar{B}$ terms leads to a tensor conductivity whose off-diagonal terms become negligible when

$$q_e B/m_e \ll \nu .$$

The collision (diffusion) effects effectively dominate the Lorentz force effects at values of ν lower than those at which the collision effects dominate the electric-field-generated particle motion. Moreover, one could not keep to the simple scalar form of equation (8) if one kept the static $\bar{B}$ field effect.

To simplify the grad p_α term, one assumes that there is an instantaneous linear change in n_α with change in p_α, so that

$$\partial p_\alpha/\partial x = m_\alpha U_\alpha^2 \, \partial n_\alpha/\partial x ,$$

where U_α is referred to as the sound speed for species α. This assumption cuts down the number of variables and eliminates the need for an additional equation such as energy conservation.

Regarding the partial pressures and related temperatures, by the definitions of pressure and temperature in terms of momentum flux and average random kinetic energy, $p_\alpha = n_\alpha kT$, where k is Boltzmann's constant. In the present problem, there are both newly formed, as well as "old," secondary electrons in the plasma. The initial energy and effective temperature of the new secondaries are greater than those of the older electrons that form the bulk of the plasma after the initial instants. However, Baum[4] has shown that the new secondaries reach the overall background temperature in times $\sim 10^{-9}$ s, so that in this analysis it is reasonable to assign to the electrons a single temperature and pressure that will extend over a range of ~0.1 s.

The source term S for secondaries is related to the high-energy electron current on the assumptions that each high-energy electron is the source of υ secondaries and that the secondaries that pass a given point z were produced in a region between z and z − ζ, provided z > ζ. Then $S = \upsilon J/(q\zeta)$. This is the procedure used, for example, by Kompaneets and by Gilinsky,[5] who take $\zeta \sim 1$ m for air at sea level and $\upsilon \sim$ (primary electron energy in electronvolts/33.

For the modification of this term by the material wall, a term S_{wall} represents the deposition rate (number per unit volume per second) of electrons generated within the material and deposited in the air region. Thus, placing z = 0 at the boundary,

$$S\,(t,z) = \begin{cases} \dfrac{\upsilon J}{-q\zeta} & z \geq \zeta \\[2ex] \dfrac{\upsilon J}{-q\zeta} + S_{wall}, & z = 0 \text{ (case (a))} \\[2ex] \dfrac{\upsilon J}{-q\zeta} + S_{wall}, & 0 \leq z < \zeta \text{ (case (b))} \;. \end{cases} \qquad (9)$$

---

[4] *C. E. Baum, Electron Thermalization and Mobility in Air, EMP Notes 2-1, TN12 (1973).*

[5] *V. Gilinsky, The Kompaneets Model for Radio Emission from a Nuclear Explosion, Rand Corporation, Report RM-134 (1964); also EMP Notes 2-2, TN 36 (1973).*

S_{wall} represents the emission of secondary electrons from the material surface into the plasma as shown by Burke et al.[6] The emission, due to high-energy primary radiation, of secondary electrons with energies below 50 eV is proportional to the incident energy flux and the material stopping power and is independent of the particular type of high-energy source whether photon (x or γ ray), 10-MeV electrons, or 0.1- to 1-keV electrons. Therefore, these sources can be lumped together in an expression for S_{wall} that will be proportional to equation (1). Additional secondaries produced by plasma electrons incident on the wall can be allowed for by introduction of an "effective reflection factor" η for plasma electrons, which has a magnitude greater than unity. Both S_{wall} and η can be determined for a number of metal surfaces.[6] Other data are given in Seiler[7] and in Bruning.[8]

The extreme, $S_{wall} = 0$, would correspond to when in the material, none of the secondaries are generated with energy exceeding the surface work function. This is the extreme considered by Longmire[3] and by Baum[9] in their rough analyses of boundary layer effects.

The secondary current is

$$J_s = -q\left(n_e u_e + n_- u_- - n_+ u_+\right) . \tag{10}$$

---

[3]C. L. Longmire, *Direct Interaction Effects in EMP, Air Force Weapons Laboratory Interaction Notes EMP 305 IN 69, Section 5 (1974).*

[6]E. A. Burke, J. A. Wall, and A. R. Frederickson, *Radiation Induced Low Energy Electron Emission from Metals, IEEE Trans. Nucl. Sci., NS-17 (September 1970), 193-199.*

[7]H. Seiler, *Some Current Problems Concerning Secondary Electron Emission, Angew. Phys., 22 (1967), translated in AFCRL Report 68-0460 (September 1968).*

[8]H. Bruning, *Physics and Applications of Secondary Emission, Pergamon Press, London (1954).*

[9]C. E. Baum, *Radiation and Conductivity Constraints on the Design of a Dipole Electric Field Sensor, EMP Notes 1-1, SSN15 (1965).*

This current plus the primary current (eq (1)) determines the electric field E, which in turn is needed to compute the u_α on the right-hand side of equation (8). Thus, equations (4) to (8) must be solved simultaneously for the seven quantities, u_α, n_α, and E in the plasma.

2.4 Electromagnetic Fields in the Material and Boundary Condition on Fields

The evolving electric field on the material side of the boundary must be considered so that equations (4) to (8) can be solved. The value of this field at the boundary x = 0 provides boundary conditions for the electric field in the plasma. Specifically, if ρ_s represents surface charge on the interface z = 0, the following jump conditions relating fields, current densities, and surface charges must hold on z = 0:

$$\varepsilon E_{material} - \varepsilon_0 E_{plasma} = \rho_s \tag{11}$$

$$\sigma E_{material} - \left(J + J_s\right)_{plasma} = \frac{\partial \rho_s}{\partial t} . \tag{12}$$

Subtracting the time derivative of equation (11) from equation (12) leads to a boundary condition that does not contain ρ_s explicitly:

$$\left(\sigma E - \varepsilon \frac{\partial E}{\partial t}\right)_{material} = \left(J + J_s - \varepsilon_0 \frac{\partial E}{\partial t}\right)_{plasma} . \tag{13}$$

To find the field in the material, one assumes that in the material, σ, ε, μ, and γ are known and constant in time and space. Then Maxwell's equations (cf. eq (3)) become

$$\frac{\partial E}{\partial t} = -\varepsilon^{-1} \left(\bar{J} + \sigma \bar{E}\right) . \tag{14}$$

This equation is readily solvable when its Laplace transform is taken in time. To do this, one writes the transforms of J(t) as $\tilde{J}(s)$, etc.

Then from equation (2),

$$\tilde{J}(s) = \tilde{J}_o(s)\exp(-\delta z) \tag{15}$$

where $\delta = \gamma + s/v$, with $v = (\mu\varepsilon)^{-\frac{1}{2}}$. Then the transform of equation (14) becomes

$$\left(\frac{s}{v^2}\right)\tilde{E} + \mu\sigma\tilde{E} = -\mu\tilde{J}_o\exp(-\delta z) \ . \tag{16}$$

Solving this algebraic equation for E and taking the inverse transform gives

$$E(t) = \frac{\exp(-\gamma z)}{2\pi i\varepsilon}\int_C \frac{\tilde{J}_o(s)\exp(su)}{s + \sigma/\varepsilon}\,ds \tag{17}$$

where the contours C in the complex s plane extends from $c - i\infty$ to $c + i\infty$ to the right of all poles of the integrand, and $u = t - z/v$.

To evaluate E(t) requires a specific form for $J_o(t)$. In particular if equation (2) is used for $J_o(t)$, straightforward integration gives (with e = 2.718 . . .)

$$\tilde{J}_o(s) \equiv J_m\int_0^\infty \exp(-st)[(t/\tau)\exp(1-t/\tau)]dt = J_m e\tau(1 + s\tau)^{-2} \ . \tag{18}$$

Inserting equation (12) into equation (11) and expanding the integrands about $s = -\sigma/\varepsilon$ and $s = -\tau^{-1}$ shows that simple poles are at these values of s. Then applying the Cauchy residue theorem yields for the field in the material

$$E(z,t) = eJ_m\exp(-\gamma z)\left[\frac{\exp\left(-\frac{u}{\tau}\right)}{\sigma\tau - \varepsilon}\left(u - \frac{\varepsilon\tau}{\sigma\tau - \varepsilon}\right) - \frac{\varepsilon\tau\exp\left(-\frac{\sigma u}{\varepsilon}\right)}{(\sigma\tau - \varepsilon)^2}\right] . \tag{19}$$

For the boundary condition equation (13), one needs

$$\left.\frac{\partial E}{\partial t}\right|_{z=0} ,$$

which in this case is

$$\left.\frac{\partial E}{\partial t}\right|_{z=0} = eJ_m \left[\frac{\exp\left(-\frac{t}{\tau}\right)}{\sigma\tau - \varepsilon} \left(1 - \frac{t}{\tau} - \frac{\varepsilon}{\sigma\tau - \varepsilon}\right) - \frac{\sigma\tau \exp\left(-\frac{\sigma\tau}{\varepsilon}\right)}{\left(\sigma\tau - \varepsilon\right)^2} \right]. \tag{20}$$

2.5 Boundary Conditions on Densities, Charges, and Currents

Besides equation (13), additional conditions are imposed on the equations to be solved. Thus, n_α, u_α, and E are zero at any point before their having been reached by the primary current; that is,

$$u_\alpha = n_\alpha = 0 \text{ for } t \leq \frac{z}{c} . \tag{21}$$

Far from the boundary, charge is neutral:

$$\lim_{z \to \pm\infty} N_+ = \lim_{z \to \pm\infty} \left(n_- + n_e\right) \tag{22}$$

where the + applies to case (b) and the - to case (a)(fig. 1).

At the boundary $z = 0$, one may assume that practically all plasma ions incident on the material are neutralized. *A priori*, one expects this to be valid for the temperatures and electric-field conditions that develop, but this assumption can be checked for applicability and, if necessary, dropped later. Quite detailed information on neutral and ion impact phenomena is summarized by Kaminsky.[10]

Reflection of plasma electrons at $z = 0$, as well as production of secondaries due to the incident plasma electrons, can be handled by introducing an effective reflection coefficient η, which may exceed one

---

[10] *M. Kaminsky, Atomic and Ionic Impact Phenomena on Metal Surfaces, Springer, Berlin (1965).*

(secondaries due to incident plasma electrons were not included in S_{wall}). The reason for separating out the two sources of secondaries is that they differ in time behavior; any due to plasma electrons are not generated with the same time behavior as in equation (1). If the production of such secondaries is negligible, then $\eta < 1$.

When $\eta < 1$ and incident ions are neutralized, the signs of the boundary values that u_α can achieve are affected. From the basic statistical theory of plasmas, u_α is the average velocity value that would result from averaging velocity over all possible values by use of the appropriate particle distribution function. Subject to the above assumptions, this average value must correspond to a net flux of each species into the wall. Hence, at z = 0,

$$u_\alpha \cdot \hat{n} \leq 0 \qquad (23)$$

where $\hat{n}$ represents the unit normal pointed out of the material. One may go somewhat further in special cases. Thus, fixing the time origin t = 0 as the instant that the leading edge of the primary electron pulse reaches z = 0,

$$u_\alpha(0,0) = 0 \text{ (case (b))} \qquad (24)$$

and

$$\left.\begin{array}{ll} u_+(t,0) = 0 & \text{(case (b))} \\ \bar{u}_+(t,0)\ \hat{n} = 0 & \text{(case (a))} \end{array}\right\} E > 0 . \qquad (25)$$

Equation (25) follows from the fact that all + ions originate in the plasma and do so with zero z-directed velocity. They are subsequently accelerated to the right for E > 0. In case (a) (air on the left), all the particles at the wall are clearly moving into the wall. In case (b) (air on the right), the only + particles available at z = 0 are the newly formed ones with zero z velocity.

3. INTEGRATION OF THE EQUATIONS

3.1 The Special Mathematical Form of the Equations

The conservation equations (5) to (8) form a quasi-linear hyperbolic system. One can put the system in a form suitable for integration by the "method of characteristics," by considering the three families of curves C_α defined in terms of arc lengths

$$\frac{dz}{ds_\alpha} = u_\alpha \; , \quad \frac{dt}{ds_\alpha} = 1 \; , \tag{26}$$

that is,

$$z - u_\alpha t = \text{constant} \; .$$

The left sides of equations (5) to (8) contain total derivatives dn_α/ds_α and du_α/ds_α along the respective curves of equation (26). Curves C_α are termed characteristic curves of the differential equations (5) to (8), which may be rewritten as

$$\frac{dn_e}{ds_e} = - n_e\left(\breve{\alpha} + \breve{\varepsilon}n_+ + \frac{\partial u_e}{\partial z}\right) + S \tag{27}$$

$$\frac{dn_-}{ds_-} = - n_-\left(\breve{\beta}n_+ + \frac{\partial u_-}{\partial z}\right) - \breve{\alpha}n_e \tag{28}$$

$$\frac{dn_+}{ds_+} = n_+\left(\breve{\beta}n_- + \breve{\varepsilon}n_e + \frac{\partial u_+}{\partial z}\right) - S \tag{29}$$

and

$$\frac{du}{ds_\alpha} = \frac{q_\alpha}{m_\alpha}E - \frac{U_\alpha^2}{n_\alpha}\frac{\partial n_\alpha}{\partial z} - \nu_\alpha u_\alpha \; . \tag{30}$$

3.2 First Iteration for n_α

The equations can numerically be integrated forward in time. For convenience, assume that the t,z plane is covered by a mesh of lines

$$t = i\Delta t, \ z = j\Delta z; \ i \text{ and } j = 0, \pm 1, \pm 2, \ldots .$$

Point P at a node of the mesh is denoted by P_{ij}. Functions f(t,z) evaluated at specific points P are written f_p, or if P is a node ij, they are written also by f_{ij}.

At a point P where u_p is assumed known, the characteristics are approximated by the straight lines

$$z - u_{\alpha p} t = \text{constant} = j\Delta z - u_{\alpha p} \cdot i\Delta t \qquad (31)$$

in the range

$$(i - 1)\Delta t \leq t \leq i\Delta t .$$

For convenience, these straight lines (which are tangents to the characteristic curves) are called characteristic lines. Denote the intersections of these lines with $t = (i - 1)\Delta t$ by A_α (fig. 3). Then in terms of prior values, as first estimates of $n_{\alpha p}$,

$$n_{\alpha p}^{(1)} \simeq n_{\alpha A_\alpha} + \left(\frac{dn_\alpha}{ds_\alpha}\right)_{A_\alpha} \cdot \overline{A_\alpha P} \qquad (32)$$

where $\overline{A_\alpha P}$ denotes the length of the line segment $A_\alpha P$.

The prior values $n_{\alpha A_\alpha}$ are assumed known from the previous integrations. The prior steps will have provided $n_{\alpha(i-1)j}$, from which $n_{\alpha A_\alpha}$ can be determined by interpolation. For equation (32), the

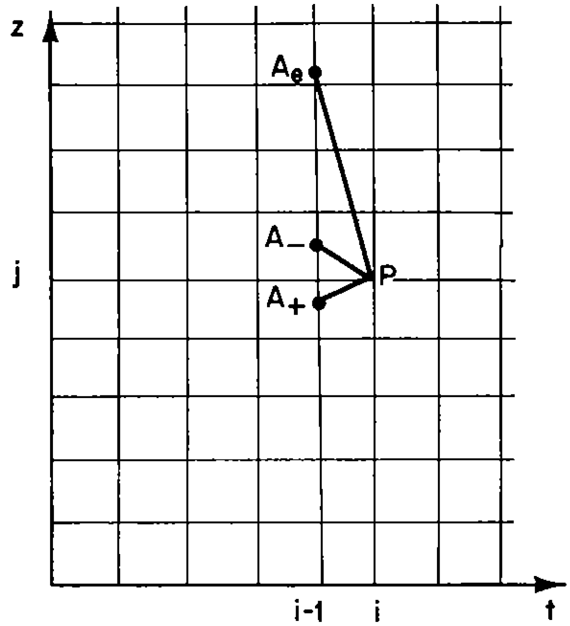

Figure 3. Characteristic lines and points A_α.

derivatives are taken when the right sides of equations (27) to (30) are evaluated by use of the same u_α value as in equation (26). The source terms S_p are given by equation (9).

3.3 Determination of u

The integration discussion so far has been predicted on knowing values of $u_{\alpha p} \equiv u_{\alpha ij}$. These quantities may be found in terms of values on $t' = (i - 1)$ by integration along the characteristic lines. A possible procedure (fig. 4) is to begin with known values $u_{(i-1)k}$ and to integrate equation (30) along the characteristic lines of equation (31) to obtain

$$u_{\alpha B_\alpha (k)} = u_{\alpha (i-1) k} + \left(\frac{du_\alpha}{ds_\alpha}\right)_{(i-1) k} \cdot \overline{P_{(i-1)k} B_{\alpha (k)}} \quad (33)$$

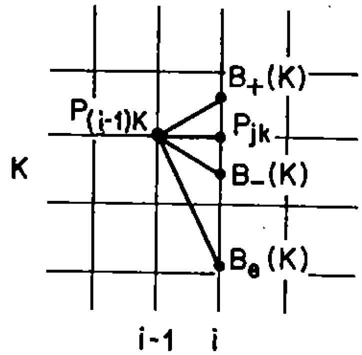

Figure 4. Characteristic lines and points $B_\alpha(k)$.

The points $B_\alpha(k)$ are the intersections of the characteristic lines of equation (31) that pass through (i-1,k) with the time line $t = i\Delta t$. Equation (33) must be applied for at least two values of k, say $k_{\alpha 1}$ and $k_{\alpha 2}$, for each species α; $k_{\alpha 1}$ and $k_{\alpha 2}$ are chosen so that the z coordinates of $B_\alpha(k_{\alpha 1})$ and $B_\alpha(k_{\alpha 2})$ bracket the value $j\Delta z$. Then $u_{\alpha ij}$ can be found by interpolation from the values $u_{\alpha B(k_{\alpha 1})}$ and $u_{\alpha B(k_{\alpha 2})}$. In each application of equation (33), the right side of equation (30) is used for the derivative du_α/ds, and the required quantity $\partial n_\alpha/\partial z$ is obtained by differencing along the line $t = (i - 1)$. The quantity $E_{(i-1)k}$ needed in equation (33) is found from prior values by use of equation (35).

3.4 Second Iteration for n_α

Once $n_{\alpha p}$ has been determined, an improved value may be obtained from the formula

$$n_{\alpha p}^{(2)} \simeq n_{\alpha A_\alpha} + \left[\left(\frac{dn_\alpha}{ds_\alpha}\right)_{A_\alpha} + \left(\frac{dn_\alpha}{ds_\alpha}\right)_P\right] \frac{\overline{A_\alpha P}}{2} , \qquad (34)$$

where now the value of $\left(dn_\alpha/ds_\alpha\right)_P$ is computed from the right sides of equations (27) to (29) by use of $n_{\alpha p}^{(1)}$ from equation (32).

3.5 Electric Field $\bar{E}$

The electric field $\bar{E}$ is found by stepwise integration along the characteristic z = constant. At each step, application of equation (4) gives

$$E_{ij}^{(1)} = E_{(i-1)j} + \frac{\Delta t \left(J_{(i-1)j} + J_{s(i-1)j}\right)}{\varepsilon_o}$$

where, via equation (10),

$$J_{s(i-1)j} = e\left(n_e u_e + n_- u_- - n_+ u_+\right)_{(i-1)j} \; . \qquad (36)$$

Equation (35) is used in computing $\left(du_\alpha/ds_\alpha\right)_{(i-1)k}$ to be inserted in equation (33). Iteration can provide an improved E_{ij}, once the quantities $n_{\alpha ij}$ and $u_{\alpha ij}$ are determined. Thus,

$$E_{ij}^{(2)} = E_{(i-1)j} + \left(\frac{\Delta t}{2\varepsilon_o}\right)\left(J_{(i-1)j} + J_{ij} + J_{s(i-1)j} + J_{sij}\right) \; . \qquad (37)$$

3.6 Boundary and Initial Computations

3.6.1 Case (b)

In case (b), at t = 0, the plasma formation from nonionized air just begins. The plasma variables are all zero for z > ct, and data for the region z > ct shown shaded in figure 5 must be determined.

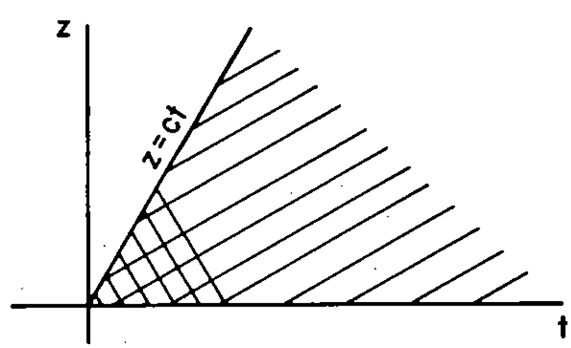

Figure 5. Integration region for positive times.

To get started, one can work with boundary value data on $z = 0$ and starting data on $z = ct$. On $z = ct$, except at $t = 0$, $u_\alpha = 0$; then the characteristics intersecting $z = ct$ are all horizontal, and integrations beginning at $z = j\Delta z$ yield data at the next node to the right.

On the boundary $z = 0$, one assumes that the initial values $u_{+00} = u_{00} = 0$ and that u_{e00} is determined by the energy distribution of the electrons contributing to S_{wall}. Then at $z = 0^+$ and $t = 0^+$, since $J_s = J = 0$, the boundary condition of equation (13) yields

$$\left.\frac{\partial E}{\partial t}\right|_{00} = - \frac{1}{\varepsilon_0} \left(\sigma E + \varepsilon \frac{\partial E}{\partial t}\right)_{\text{material}} \Bigg|_{\substack{z=0^- \\ z=0}} .$$

Then using

$$E_{00} \simeq \frac{1}{2} E_{10} \simeq \frac{1}{2} \left.\frac{\partial E}{\partial t}\right|_{00} ,$$

Δt in equation (30) yields first iterate values for

$$\left.\frac{du_\alpha}{ds_\alpha}\right|_{00} .$$

Likewise, the initial data including

$$S_w \Big|_{t=0}$$

yields

$$\left.\frac{dn_\alpha}{ds_\alpha}\right|_{00}$$

from equations (27) to (29). In this fashion and with the characteristics as $z = 0$ kept over the first two or three intervals, one can determine all the data at points 10, 20, and 30. Then, using these results to determine the actually nonzero slopes of the chracteristics, one can work towards increasing z and decreasing t, filling in the area shown crosshatched in figure 5 with first iterate estimates of the data.

Next, one can start on the line $z = ct$, using $n_\alpha = 0$, $u_\alpha = 0$, and $E = 0$, but $s \neq 0$. Then equations (27) to (29) permit one to determine n_e at the nearest nodes (ij) to the right of $z = ct$ and thus to get the procedures started. This action permits filling in the crosshatched area with first iterate estimates. Successive iterations should then be used to make the data compatible, to satisfy the conditions on both $z = ct$ and $z = 0$.

The boundary condition $u_+(t,0) = 0$ given by equation (24) should hold at least for early times, since $E(t,0)$ is positive up to $t = \tau$. Hence, until $t = \tau$, $u_{+i0} = 0$ must be used in the computation. Likewise, the boundary condition of equation (13) must be satisfied at all t.

At all times, E_{j0} is governed by the boundary condition of equation (13), with the secondary current density J_s computed via $u_{\alpha j0}$ and $n_{\alpha j0}$.

Computation is continued until equation (22) is adequately satisfied.

3.6.2 Case (a)

In case (a), by $t = 0$, the air has been partially ionized, and the current pulse has just reached the material surface. Hence, it is necessary to compute for some time $t = t_c < 0$, to establish the ambient plasma that is modified by air-material interface effects commencing at $t = 0$.

Thus, starting with initial values $u_\alpha = n_\alpha = E = 0$ on the lines $z = ct$ for $t < 0$ and $t = t_c$, one can follow the procedures of sections 3.1 to 3.5, filling in the shaded triangle (fig. 5), working toward the right until the data are obtained along the line $t = 0$. In this region, the time scale is expanded, compared to the time scale used in case (b), in which the line $z = ct$ was essentially vertical. Time t_c is chosen such that $|ct_c|$ is appreciably larger than the expected sheath region thickness; it must be checked *a posteriori* whether the chosen t_c indeed satisfies this criterion.

Once the values of u_α, n_α, and E are determined on $t = 0$ by integration from $t < 0$, these values can serve for the subsequent integration to fill in the data for $t > 0$, $z < 0$. In this region (fig. 6), the compressed time scale may be used, and the boundary procedures at $z = 0$ are the same as for case (b).

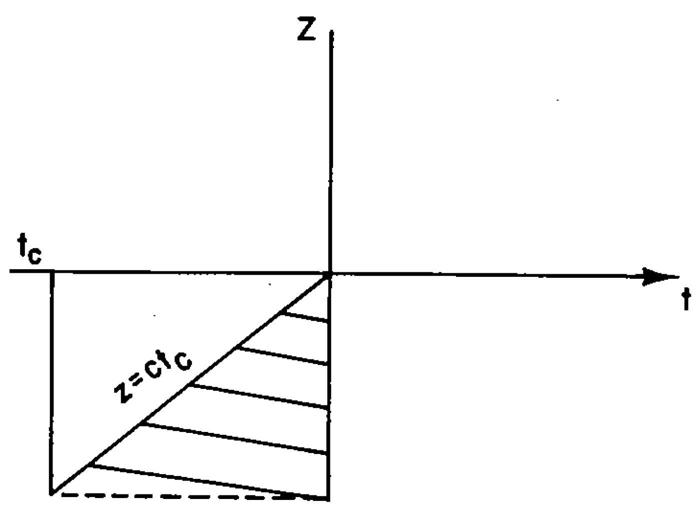

Figure 6. Integration region for negative times, case (a).

LITERATURE CITED

(1) J. Tarstrup and W. D. Heikkila, The Impedance Characteristic of a Spherical Probe in an Isotropic Plasma, Radio Science, 7 (April 1972), 493-502.

(2) J. D. Swift and M. J. R. Schwar, Electrical Probes for Plasma Diagnostics, American Elsevier, New York (1972)

(3) C. L. Longmire, Direct Interaction Effects in EMP, Air Force Weapons Laboratory Interaction Notes EMP 305 IN 69, Section 5 (1974).

(4) C. E. Baum, Electron Thermalization and Mobility in Air, EMP Notes 2-1, TN12 (1973).

(5) V. Gilinsky, The Kompaneets Model for Radio Emission from a Nuclear Explosion, Rand Corporation, Report RM-134 (1964); also EMP Notes 2-2, TN 36 (1973).

(6) E. A. Burke, J. A. Wall, and A. R. Frederickson, Radiation Induced Low Energy Electron Emission from Metals, IEEE Trans. Nucl. Sci., NS-17 (September 1970), 193-199.

(7) H. Seiler, Some Current Problems Concerning Secondary Electron Emission, Angew. Phys., 22 (1967), translated in AFCRL Report 68-0460 (September 1968).

(8) H. Bruning, Physics and Applications of Secondary Emission, Pergamon Press, London (1954).

(9) C. E. Baum, Radiation and Conductivity Constraints on the Design of a Dipole Electric Field Sensor, EMP Notes 1-1, SSN15 (1965).

(10) M. Kaminsky, Atomic and Ionic Impact Phenomena on Metal Surfaces, Springer, Berlin (1965).